Journal of Taibah University for Science

ISSN: (Print) (Online) Journal homepage: www.tandfonline.com/journals/tusc20

Enhanced anticancer effect of newly synthesised albumin-bound Fe(III)-S-Methyl-thiosemicarbazones on breast cancer cells

Ferdane Danışman-Kalındemirtaş, Serap Erdem-Kuruca, Gökçe Erdemir Cilasun, Esra Sert, Dilşad Özerkan, Tülay Bal Demirci, Bahri Ülküseven & İshak Afşin Kariper

To cite this article: Ferdane Danışman-Kalındemirtaş, Serap Erdem-Kuruca, Gökçe Erdemir Cilasun, Esra Sert, Dilşad Özerkan, Tülay Bal Demirci, Bahri Ülküseven & İshak Afşin Kariper (2024) Enhanced anticancer effect of newly synthesised albumin-bound Fe(III)-S-Methyl-thiosemicarbazones on breast cancer cells, Journal of Taibah University for Science, 18:1, 2375454, DOI: 10.1080/16583655.2024.2375454

To link to this article: https://doi.org/10.1080/16583655.2024.2375454

JOURNAL OF TAIBAH UNIVERSITY FOR SCIENCE
2024, VOL. 18, NO. 1, 2375454
https://doi.org/10.1080/16583655.2024.2375454

JTUSCI

Journal of Taibah University for Science

Taylor & Francis
Taylor & Francis Group

OPEN ACCESS Check for updates

Enhanced anticancer effect of newly synthesised albumin-bound Fe(III)-S-Methyl-thiosemicarbazones on breast cancer cells

Ferdane Danışman-Kalındemirtaş[a], Serap Erdem-Kuruca[b], Gökçe Erdemir Cilasun[c], Esra Sert[d], Dilşad Özerkan [e], Tülay Bal Demirci[f], Bahri Ülküseven[f] and İshak Afşin Kariper[g]

[a]Erzincan Binali Yıldırım University, Faculty of Medicine, Department of Physiology, Erzincan, Turkey; [b]Istanbul Atlas University, Faculty of Medicine, Department of Physiology, İstanbul, Turkey; [c]Istanbul University, Faculty of Medicine, Department of Physiology, İstanbul, Turkey; [d]Istanbul University, Health Sciences Institute, Department of Internal Medicine, İstanbul, Turkey; [e]Kastamonu University, Faculty of Engineering and Architecture, Department of Genetic and Bioengineering, Kastamonu, Turkey; [f]Istanbul Cerrahpaşa University, Faculty of Engineering, Department of Chemistry, İstanbul, Turkey; [g]Erciyes University, Education Faculty, Department of Science Education, Kayseri, Turkey

ABSTRACT

Thiosemicarbazones and their analogues are of significant interest due to their antiviral, antibacterial and anticancer properties. Recent advancements in nanoparticle-based therapeutics have enabled targeted cancer cell treatment while minimizing harm to healthy cells. This study focused on encapsulating patented N(1)-R1-salicylidene-N(4)-R2-salicylidene-S-methylisothiosemicarbazone complexes into albumin nanocarriers, creating albumin-bound Fe(III)-S-methyl-thiosemicarbazone (ALB-FeTc) nanoparticles via a novel UV-C lamp-assisted method. The nanoparticles were characterized using FTIR, UV-Vis, DLS and EDX-SEM. Cytotoxicity was evaluated in MCF-7 breast cancer cells and HUVEC cells using an MTT assay. Fluorescence microscopy and flow cytometry were employed to investigate the mechanism of cell death. The study demonstrated strong cytotoxicity of FeTcs against cancer cells, with enhanced effects observed for ALB-FeTcs. The ALB-FeTcs induced apoptosis selectively in cancer cells while sparing normal cells. These results suggest that ALB-FeTcs are promising candidates for breast cancer treatment.

ARTICLE HISTORY
Received 22 February 2024
Revised 6 May 2024
Accepted 28 June 2024

KEYWORDS
Nano albumin; Iron Thiosemicarbazone; MCF-7; breast cancer; Research&Development (R&D)

1. Introduction

The most dangerous tumor in women is breast cancer, where about fifteen percent of breast tumors have a significant overexpression of HER2, which is associated with a higher risk of recurrence and a more aggressive disease course [1]. Breast cancer survival rates have improved worldwide due to advances in early detection and treatment. According to the World Health Organization (WHO), 5-year survival rates for breast cancer vary significantly by region and stage at diagnosis. In high-income countries, for example, the 5-year survival rate for breast cancer is over 85%. In low – and middle-income countries, survival rates tend to be lower due to limited access to medical resources, late diagnosis and suboptimal treatment. Mortality rates also vary around the world, with higher rates in regions with limited access to healthcare and screening programs [2]. Despite the use of therapeutic techniques such as radiation, chemotherapy and surgery, breast cancer remains a potentially fatal disease for humans. The current study looks at the new possibilities that nanomedicine has opened up in the treatment of breast cancer. Chemotherapeutic drugs and natural products are administered via nanocarriers that both increase cytotoxicity to breast cancer cells and prevent the development of drug resistance [3].

The class of thiosemicarbazones from the di-2-pyridylketone group exhibits potent anticancer properties by binding essential metal ions such as iron (Fe(II)), copper (Cu(II)) and zinc (Zn(II)) in cancer cells and forming metal complexes. These drugs are promising when it comes to preventing the three main causes of cancer death: Tumor development, metastasis and resistance [4]. Although they are lethal to cancer cells, thiosemicarbazones tend to crystallize under normal conditions [5]. This condition can occasionally make their use as a therapeutic agent challenging. This can make their use as a therapeutic agent challenging at times. It can also be difficult for the body to excrete them as they can crystallize and solidify in the cell. Therefore, it is a challenge to find commercial samples for clinical use. In this study, we aim to facilitate the use of the highly effective thiosemicarbazones in treatment by reducing their disadvantages. On the other hand, the aim is to get the drug into the cancer cell while minimizing damage to healthy cells. In the treatment of breast

CONTACT Dilşad Özerkan dilsadokan@gmail.com

Supplemental data for this article can be accessed online at https://doi.org/10.1080/16583655.2024.2375454.

cancer, nanocarriers can provide a framework for drug delivery. Breast tumors can become more receptive to chemotherapy when treated with drugs [3].

Nanomaterials have proven to be promising tools in the treatment of cancer due to their unique properties and versatility [6]. These materials are produced using chemical or green synthesis methods and are used in a variety of ways, including drug delivery, imaging and therapy, reducing drug resistance, enhancing antitumor activity and minimizing side effects [7–13]. Protein-based nanocarriers have gained popularity over other nanomaterials because they have several advantages and can be used safely under physiological conditions. Albumin can enhance the attachment and internalization of nanomaterials by attaching to specific receptors that are overexpressed in malignant cells [14]. Various tumors overexpress the 60 kDa glycoprotein (gp60) receptor and secrete an acidic and cysteine-rich protein (SPARC) [15]. Albumin can bind to gp60 and SPARC, thoroughly enhancing the uptake of the nanocarrier and preventing albumin-based nanoparticles from excreting the drug from tumor cells [16]. In addition, it is known that albumin has a high proportion of carboxyl and amino groups, which can be used for active targeting via surface functionalization. As a result, albumin-based nanocarriers show their efficiency by reducing the efflux of the drug from the cell and, at the same time, increasing the uptake of the drug into the cell. As a result, the drug accumulates in the tumor, which can overcome anticancer drug resistance [14]. Nab-paclitaxel has also been shown to increase the binding of paclitaxel to the endothelium by 9.9-fold compared to Cremophor EL-paclitaxel, and paclitaxel are delivered 4.2 times more efficiently [16, 14].

The term "externally stimulating" refers to carriers under the control of one or more agents external to the body. These agents can modify drug release behavior, direct the carrier to a specific site, add a therapeutic approach, etc. There are reports of various forms of external stimulation systems, such as light, magnetic field, ultrasound, and others, used in cancer therapy [17–19]. The minimally invasive procedure known as photothermal therapy (PTT) raises the temperature of specific tissues by using photothermal agents (PTAs) that emit visible or non-visible light at wavelengths such as microwaves, ultrasound, or near-infrared. As cancer cells are more sensitive to high temperatures, this technique kills cancer cells while protecting healthy cells [20].

The advantages of using nanomaterials for thermal stimulation in biological systems are their absorbability, biocompatibility, small size, biodegradable solvent dispersion, and heat generation upon external stimulation [21]. A shift in synthesis for specific nanoparticles alters the absorption peak within a particular wavelength range, improving the photothermal effect and PTT quality. In addition, the biological capacity of nanostructures can be modulated, and toxicity issues can be minimized by linking nanomaterials with various surface-modifying molecules such as polymers or antibodies [22]. Another advantage of nanomaterials is their ability to direct a drug to specific body regions. This situation minimizes the required dose and enables safe drug delivery while protecting non-target tissues and cells from harmful side effects.

The present study loaded iron-bound thiosemicarbazones onto the albumin nanocarrier to form the ALB-FeTc group. We investigated the biotechnological drug potential of the thiosemicarbazones we studied at lower doses and for more extended periods to increase their efficacy and selectivity further (with minimal toxicity to healthy cells). In recent years, it has been determined that the stimulation of various nanoparticles with X-irradiation enhances their anticancer efficacy [23,24]. Therefore, it has emerged that such combinatorial therapies may be particularly effective against breast cancer. To this end, we synthesized ALB-FeTcs and investigated their cytotoxic effect on breast cancer cell lines. In contrast to the albumin nanoparticles that have already been explored, this work uses UV light to ensure that the drug is bound to the albumin in a controlled manner during the incorporation of the thiosemicarbazones into the albumin, thus controlling the size of the nanoparticles.

2. Materials and Methods

Bovine serum albumin of analytical grade was purchased in analytical grade (Sigma Aldrich) Roswell Park Memorial Institute (RPMI) (Biological et al. Number: BI01-100-1A), MTT (Invitrogen^{TM} CAS Number: DAL110), fetal bovine serum (FBS) (Serana CAS Number: SRS-FBSP-EU-002), penicillin/streptomycin (Serana CAS Number: SRRAL-002-100M), phosphate Buffered Saline (PBS) (Gibco, CAS Number: 10010023), dimethyl sulfoxide (DMSO) (Sigma CAS Number: 67-68-5), Annexin V-FITC Apoptosis Detection Kit (Sigma-Aldrich CAS Number: APOAF-20TST), 4′,6-Diamidino-2-phenylindole dihydrochloride (DAPI) (ThermoFisher CAS Number: D1306) were purchased.

2.1. Solution Preparation and Nanoparticle Synthesis

1 mL of the 0.2 g/20 mL prepared albumin solution was withdrawn and 1 mL each of the FeTcA, FeTcB and FeTcC preparations were withdrawn and sonicated in an Eppendorf tube for 30 s. The prepared solutions were then stored in a sterile atmosphere for one hour under a 30 W (Philips brand) UV-C lamp.

2.2. Characterization of ALB-FeTc Nanoparticles

2.2.1. Zeta Sizer Measurements

Zetasizer measurements were performed by DLS using the Zetasizer Nano ZS (Malvern), which uses a 4 mW He – Ne laser operating at a wavelength of 633 nm and a detection angle of 173° at room temperature. Distilled water was used as the reference liquid. Both size and surface load analyses were performed during the measurements. Samples were stored in a refrigerator at +4°C for 1 hour and measurements were performed with the Zetasizer Nano ZS device at room temperature. Each sample was measured three times and the average of the three measurements was determined [25].

2.2.2. FTIR Analyzes

The FTIR studies were performed using the BRUKER ALPHA device in diffuse reflectance mode at a resolution of 4 cm x 1. The measurement of each sample was recorded after ten scans. After the device was set up with pure water, the measurements were performed with the samples. The liquid samples were placed in the chamber under the ATR head. After the ATR head was pressed onto the sample, the measurements were performed with the device. The recorded data was analysed after smoothing [25].

2.2.3. SEM-EDX Analyzes

First, the samples were placed on amorphous lamellar glass substrates. Before use, these substrates were cleaned with detergent and plenty of distilled water. The samples were dried for one night at room temperature and under typical air conditions in a clean room. SEM-EDX studies were then performed on these samples. The surface properties of the powders were analyzed using a computer-controlled digital SEM Gemini 500. Quantitative elemental analysis was performed using an EDX spectrometer connected to the SEM [25]. Details of FeTc synthesis can be found in Supplementary Table S1 and Figure S1.

2.2.4. UV-VIS. Analyzes

The Hach Lange DR 5000 spectrophotometer measures the absorbance of the samples. Water was used as the standard for the reference part of the spectrophotometer, and the solutions prepared for the sample part were used for reference measurements in the wavelength range of 200–1100 nm [25]

2.2.5. Raman Analyzes

JASCO NSR-3100 Raman spectroscopy (with a 532 nm laser probe) was used to record the broadband Raman spectra of the Alb-FeTc nanoparticle samples. The liquid samples were placed in the sample chamber. The measurements were performed using the Raman spectroscopy instrument. The recorded data were analyzed after smoothing.

2.3. Cell Viability Test with MTT

2.3.1. Cell Culture and stabilization of cell lines

MCF-7 breast cancer and healthy HUVEC cell lines were utilized within the scope of this investigation. The cells underwent cultivation in RPMI enriched with 10% FBS, subsequent to which they were subjected to centrifugation and distributed into either 75 or 25 cm^2 flasks based on their respective densities. Following this, the cells were subjected to incubation at a temperature of 37 °C within an incubator containing a gaseous composition of 95% O_2 and 5% CO_2. The culture medium employed in this study consisted of RPMI supplemented with 10% FBS, into which 100.000 U/mL of penicillin and 100.000 g/L of streptomycin were incorporated. Passage of the cells was performed upon reaching a confluence level of 70-90%.

Cell viability calculation was made according to the following formula:

$$\begin{aligned}\text{Total cells} = {} & \text{Cells counted} \\ & \times \text{ Dilution factor} \\ & \times \text{ Total volume } \times \text{ 10,000.}\end{aligned}$$

2.3.2. Determination of Cytotoxic Concentrations (IC_{50})

When MCF-7 and HUVEC cells were 70-90% confluent, they were scraped from the bottom of the flask with trypsin and stained with trypan blue, and their viability was assessed by counting the cells. In 96-well plates, 90 µl of the cells were seeded at a cell count of 10^4 per milliliter. After 72 hours of incubation, chemicals were added at a dosage of (0.05, 0.5, 1, 2 µg/ml) and the MTT assay [26] was performed on the cells. After 72 hours of incubation, an MTT solution of 0.5 mg/ml prepared in PBS was applied to the cells and after 4 hours of incubation in the dark at 37 °C in an incubator, 100 µl of DMSO was added to each well of the 96-well plate to dissolve the cells. The ELISA device read the cells at 570 nm. Each experiment was performed at least three times. The IC_{50} value was calculated using GraphPad Prism5 statistical software.

2.4. Flow Cytometry Analysis for Apoptosis Detection

The Annexin V-FITC Apoptosis Detection Kit was used. MCF-7 cells (5×10^5), untreated and treated with ALB-FeTcs for 72 hours at 37 °C and 5% CO_2, were harvested from the 6 wells at the end of the incubation period and placed in fluorescence-activated cell sorting (FACS) tubes. Cold culture medium or PBS was used to wash the cells. It was centrifuged at 4 °C for 5 minutes at 1800rpm. The supernatant was removed and the suspended cells were kept in 1x binding buffer at room temperature. The tubes were kept cold. To 100 µL of the cell suspension, 1 µL of Annexin V-FITC solution and 2.5

μL of dissolved propidium iodide (PI) were added. The tubes were placed on ice and incubated for 15 minutes in the dark. 400 μL of the 1x binding buffer was added and mixed thoroughly on ice [27]. The Kaluza analysis program examined the cell sample using the Beckman Coulter Navios Flow Cytometry device.

2.5. DAPI Staining for Fluorescence Microscope Imaging

DAPI is a dye that can be used as a tool to visualize nuclear changes and assess apoptosis. DAPI binds strongly and selectively to the minor groove of adenine–thymine regions of DNA [28]. Coverslips were disinfected with alcohol and flame before being put on sterile 6-well plates. MCF-7 cells were sown at a density of 10^5 per milliliter. Substance doses at IC_{90} levels were applied and incubated for 24 hours at 37°C in a 5% CO_2 incubator. The medium was removed after 24 hours and rinsed with PBS. Each cell was fixed in alcohol for 15 min. After washing with PBS, it was incubated in the dark for 30 min. with DAPI (1 μl stock DAPI dye diluted in 5 ml PBS). PBS was used to rewash the stained areas after staining. The coverslips were placed on the slide, and images were taken using a Nikon Eclipse Ts2 immunofluorescence microscope.

3. Results And Discussion

It is known that thiosemicarbazone class compounds have bioactivity against some types of cancer [29]. In particular, protein-based nanocarriers have many favorable properties compared to other nanocarriers and can be used safely in the biological environment, so they are preferred over other nanomaterials. The synthesis of albumin-based thiosemicarbazone nanoparticles is aimed to create treatments with fewer side effects and to provide targeted effects in cancer cells. Another reason for choosing the protein albumin nanocarrier is that it is FDA-approved, can be explicitly directed to cancer cells via the gp60 and sparc receptors in the cell while carrying the drug, and albumin does not have its toxicity [14]. Albumin and its nanoparticles can be used in the diagnosis and therapy of various diseases, such as various kinds of cancer [30–32]. In light of this information, our study studied modified forms of albumin-based nanoparticles as nano drugs on MCF-7 breast cancer cells. Nanoparticle-based, especially protein-based nanoparticles, attract attention because they can be used safely thanks to their biocompatibility. In our study, the iron form of the albumin-based nanoparticle was modified to bind FeTcs to albumin in a regulated manner during the integration of the thiosemicarbazones into albumin, UV light was used, and the anticancer effect of ALB-FeTcs was investigated.

The size of the nanocarrier system plays a crucial role in drug delivery, as the nanoparticles up to 400 nm preferentially accrue in the tumor microenvironment via the "enhanced permeability and retention (EPR)" effect [33]. The drug-loaded albumin nanoparticles are transparent and have a diameter of hundreds of nm (usually less than 200 nm). A 0.22μm filter is used to manage the size of the nanoparticles and sterilize the formulation, removing impurities and microorganisms. After that, nanoparticles are lyophilized (without any cryoprotectant) to produce solid powders. The distribution can be reproduced by adding water or saline to solid nanoparticles [34]. In this work, the size distribution of the nano-sized FeTcA sample begins at 58.75 nm and extends to 190 nm, as shown in Table 1 and Figure 1. While the average particle size was estimated to be 101.9 nm, the Derived Count Rate was 4412 (PDI: 0.147). Similarly, the FeTcB sample's size distribution ranged from 43.82 nm to 164.2 nm. While the average particle size was estimated to be 75.57 nm, the Derived Count Rate was as high as 2836 (PDI: 0.256). The FeTcC sample's size distribution ranged from 50.75 nm to 164.2 nm. The average particle size was roughly 84.62 nm, although the Derived Count Rate was as high as 4490 (PDI: 0.178). This finding indicates a high quantity of albumin + FeTc in the environment.

According to Bhushan et al. 2015 [35], the noticeably more significant zeta potential may cause the stability of the NPs. The fact that the value is inside the stable range indicates that the creation of nanoparticles promotes the development of stable systems. Furthermore, by preventing the nanoparticles from clumping together in the colloid form, the electrostatic repulsive force between their negatively charged surfaces provides the colloidal solution with excellent stability [36]. The surface potential distribution of the nanoscale FeTcA, FeTcB, and FeTcC samples is also provided in Table 1. The FeTcA sample's surface potential was – 21 mV (conductivity (mS/cm): 1.37). The FeTcB sample's surface potential was – 16.2 mV (conductivity (mS/cm): 1.34). The FeTcC sample's surface potential was – 18 mV (conductivity (mS/cm): 1.40), as shown in Figure 2. Generally, the conductivity, PDI values, and particle dispersion of the generated nanoparticle solutions did not significantly alter. The size distribution of the particles is similar despite minor differences in the average particle size.

Figure 3 displays nanoparticle images captured by SEM. There were no grains bigger than 100 nm. Dispersion was also seen in other samples; however, FeTcA nanoparticles remained spherical. Naturally, even though the structures are chemically identical, there is still an impact from the irregularity of the solvent evaporating out of the surrounding environment. These outcomes support the DLS findings.

Nanostructure size is the most important for penetration and exhibiting cytotoxic performance in tumor sites. Cui et al. 37 [37] investigated the impact of replaceable albumin nanoparticles, which they synthesized in

Table 1. DLS (dynamic light scattering) results

Samples	Average Particle Size (nm)	Size Distribution (nm)	Zeta Potential (mV)	Conductivity (mS/cm)	PDI
Alb-FeTcA	101.9	58.75-190	−21	1.37	0.147
Alb-FeTcB	75.57	43.82-164.2	−16.2	1.34	0.256
Alb-FeTcC	84.62	50.75-164.2	−18	1.40	0.178

Note: Alb-FeTc: Albumin-Bound Fe(III)-S-Methyl-Thiosemicarbazones nanoparticles. The other molecular structures (Alb-FeTcA, Alb-FeTcB, and Alb-FeTcC) are defined in the supplementary section.

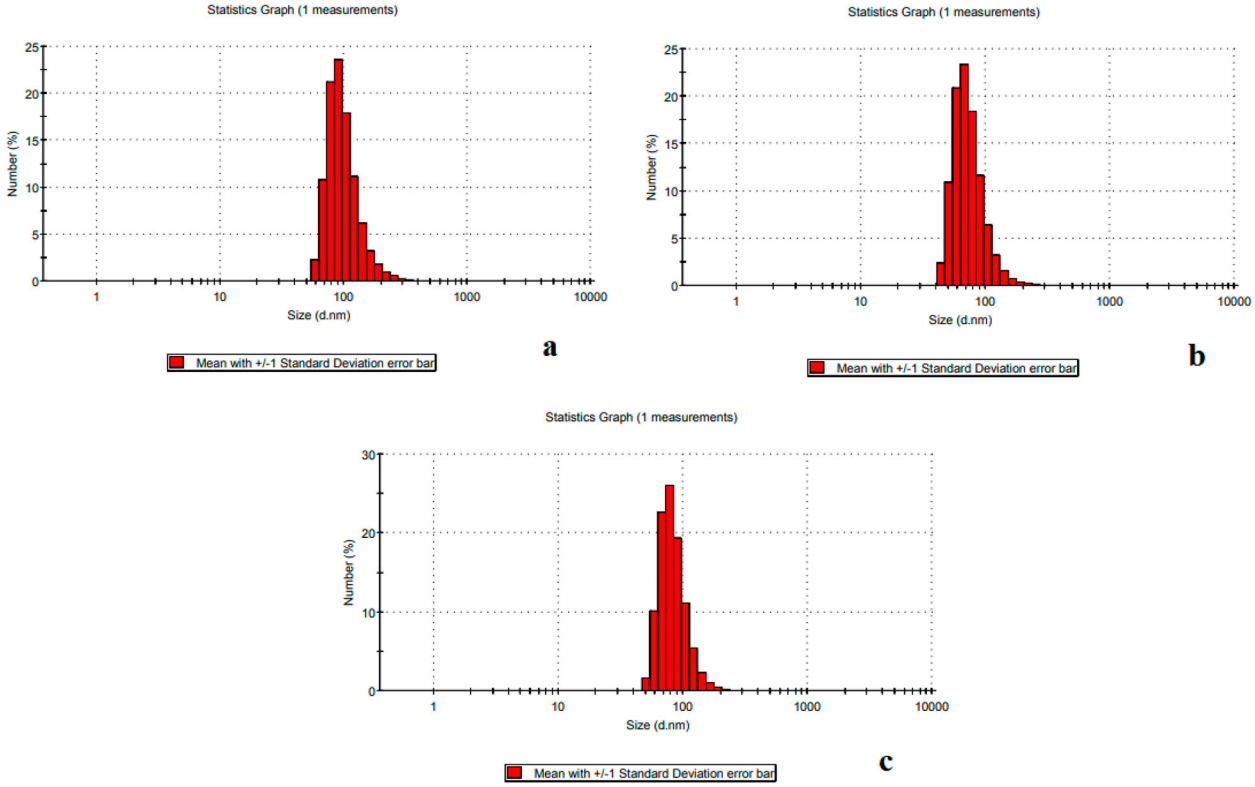

Figure 1. DLS (dynamic light scattering) graphics of **(a)** Alb-FeTcA, **(b)** Alb-FeTcB, **(c)** Alb-FeTcC. Number% is the nanoparticle percentage in the distribution. The size is a nanometer scale.

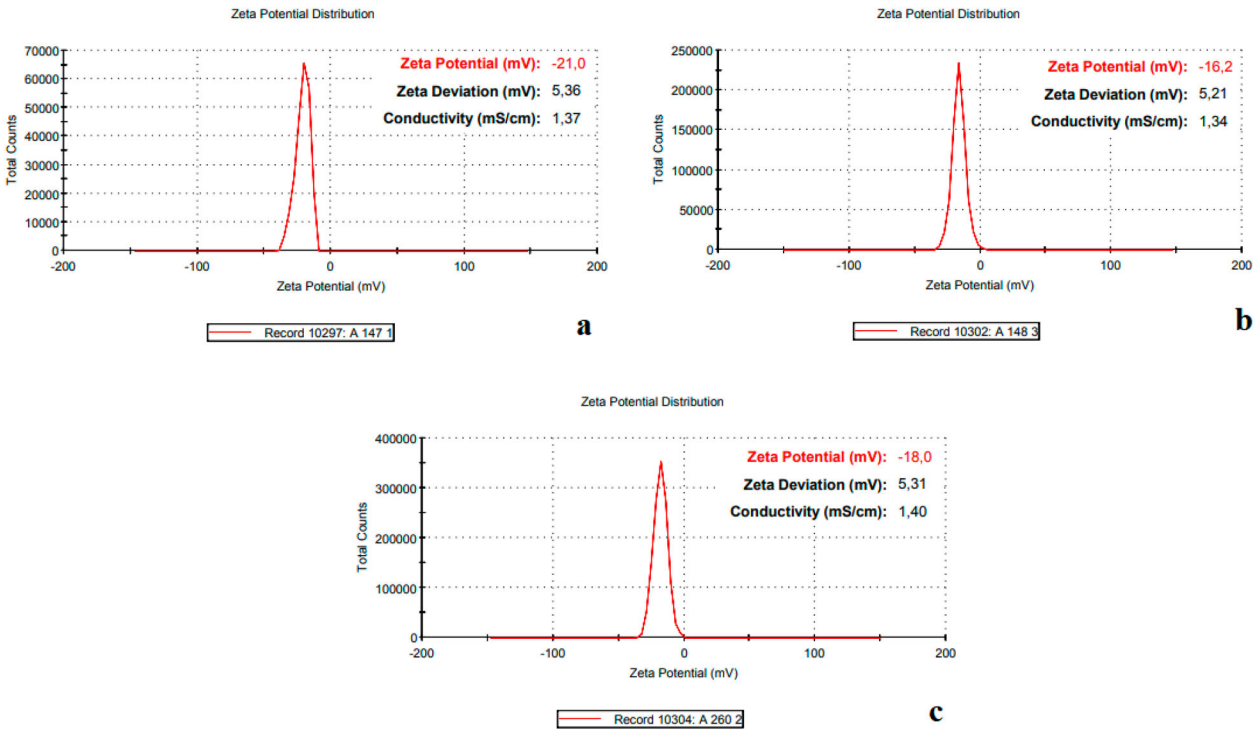

Figure 2. Zeta sizer of **(a)** Alb-FeTcA, **(b)** Alb-FeTcB, **(c)** Alb-FeTcC. Zeta potential is given as mV. Conductivity is given as mS/cm.

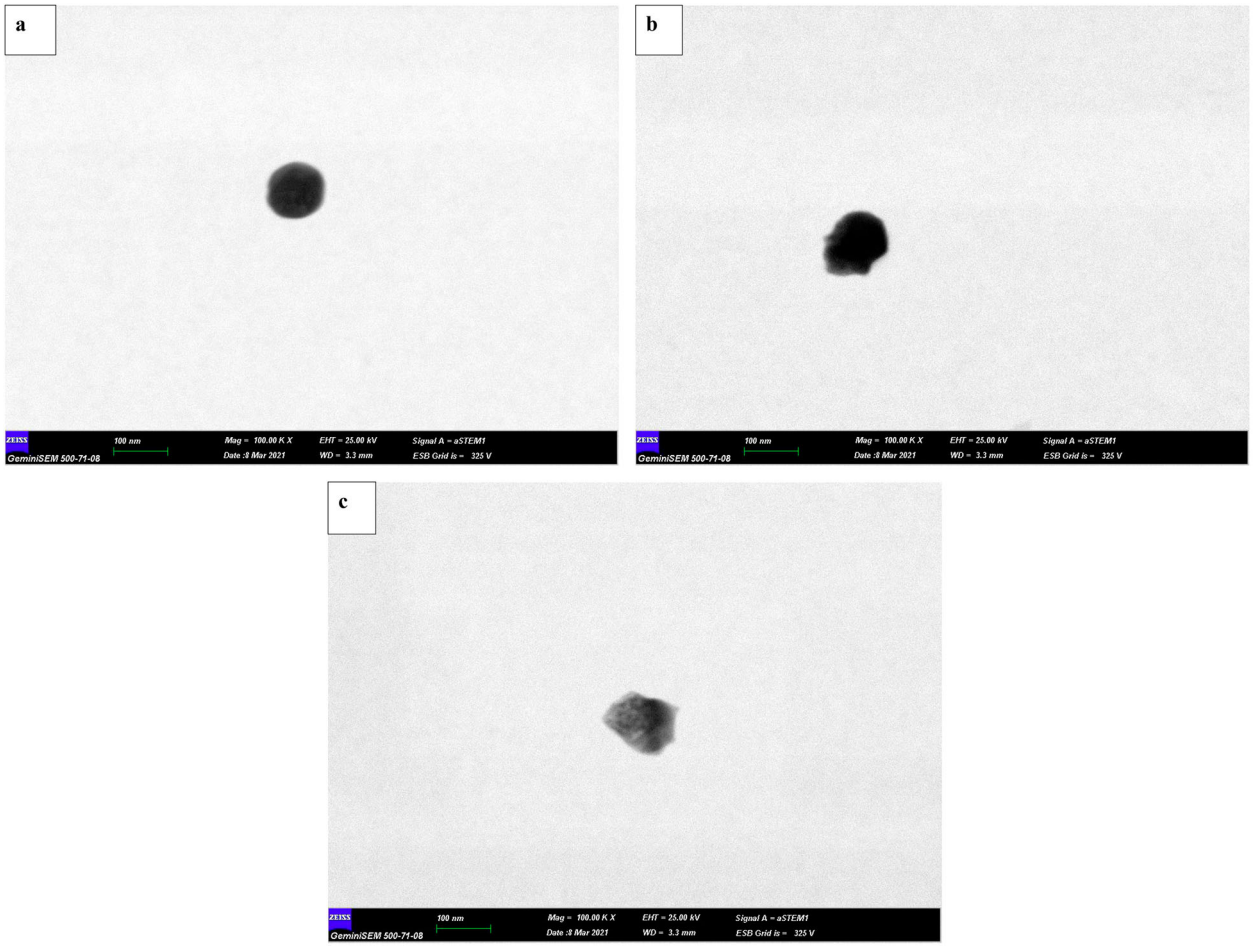

Figure 3. STEM images of **(a)** Alb-FeTcA, **(b)** Alb-FeTcB, **(c)** Alb-FeTcC. STEM images of the samples are at a 100 nm scale. Magnitude: 100.00 KX, EHT: 25.00 kV.

various forms, on 3D and *in vitro* melanoma spheroid tumors. They discovered that larger ALB-NPs had a faster 24-hour penetration rate into spheroids, which led to a faster cytotoxic effect. However, within the first 24 hours, tiny albumin nanostructures exhibit a latent phase in cell toxicity. As the 96-hour mark drew near, they discovered that the drug combinations they had administered exhibited increased cytotoxic activity, most likely as a result of the release profile. This finding suggests that albumin nanostructures can be employed as a versatile chemotherapeutic medication by varying their time and spatial dimensions.

Table 2 and Figure 4 contain EDX analyses. The percentage amounts of the base material and coating metals on which the samples were dropped are not included in the table. As can be seen, there was no substantial change in the atomic ratios of C%, O%, S%, N%, and Cl% among all samples. As a result, organic components in albumin's structure contribute to the atomic ratio. Iron, the heavy element in the middle, plays a critical role in such macromolecules. Even if the change is still minimal, it is clear that Alb-FeTcC has the most significant iron content and, thus, the most substance in the nanostructure.

The UV-VIS spectra of the samples are displayed in Fig. 5a. An emission peak at 320 nm and a particular

Table 2. EDX (energy-dispersive X-ray spectroscopy) analyzes of FeTcs

	C%	O%	S%	N%	Cl%	Fe%
Alb-FeTcA	62.08	17.39	3.01	16.22	1.05	0.25
Alb-FeTcB	61.41	17.18	2.90	17.14	1.10	0.27
Alb-FeTcC	61.62	17.51	3.26	16.17	1.11	0.33

Note: Atomic percentage values of the elements are given in the table.

Table 3. The IC_{50} Values (μg/mL) of FeTcA, FeTcB, FeTcC, and ALB-FeTcA, ALB-FeTcB, ALB-FeTcC on HUVEC and MCF-7 cells.

	The IC_{50} Values (μg/mL)	
Compounds	MCF-7	HUVEC
FeTcA	0.646 ± 0.101	1.181 ± 0.14
FeTcB	0.712 ± 0.11	1.154 ± 0.11
FeTcC	0.607 ± 0.09	1.381 ± 0.2
ALB-FeTcA	0.141 ± 0.06	0.933 ± 0.09
ALB-FeTcB	0.197 ± 0.08	0.940 ± 0.13
ALB-FeTcC	0.247 ± 0.07	1.037 ± 0.107

maximum absorption peak at 244 nm was noted at high albumin concentrations in an aqueous medium (0.2 g/20 mL). The literature claims these peaks change based on the albumin's conformation and surroundings [38]. When the medication was attached to albumin, the emission peak, which belonged to the β-sheet structure of albumin at 240 nm, either stayed below or was dampened. The literature states that whereas the n-π^* and π-π^* electronic transitions of thiosemicarbazones

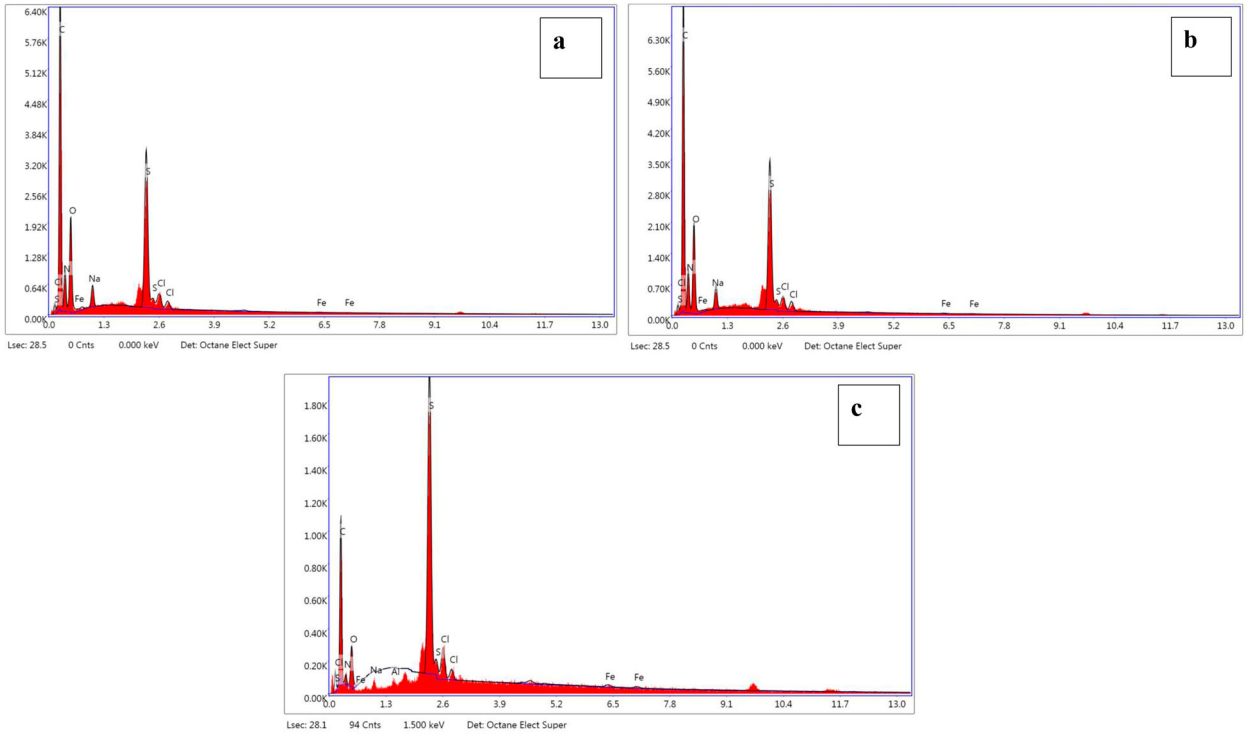

Figure 4. EDX analysis of the samples **(a)** Alb-FeTcA, **(b)** Alb-FeTcB, **(c)** Alb-FeTcC. 20 kV, resolution: 127.9 eV, magnitude: 1093.

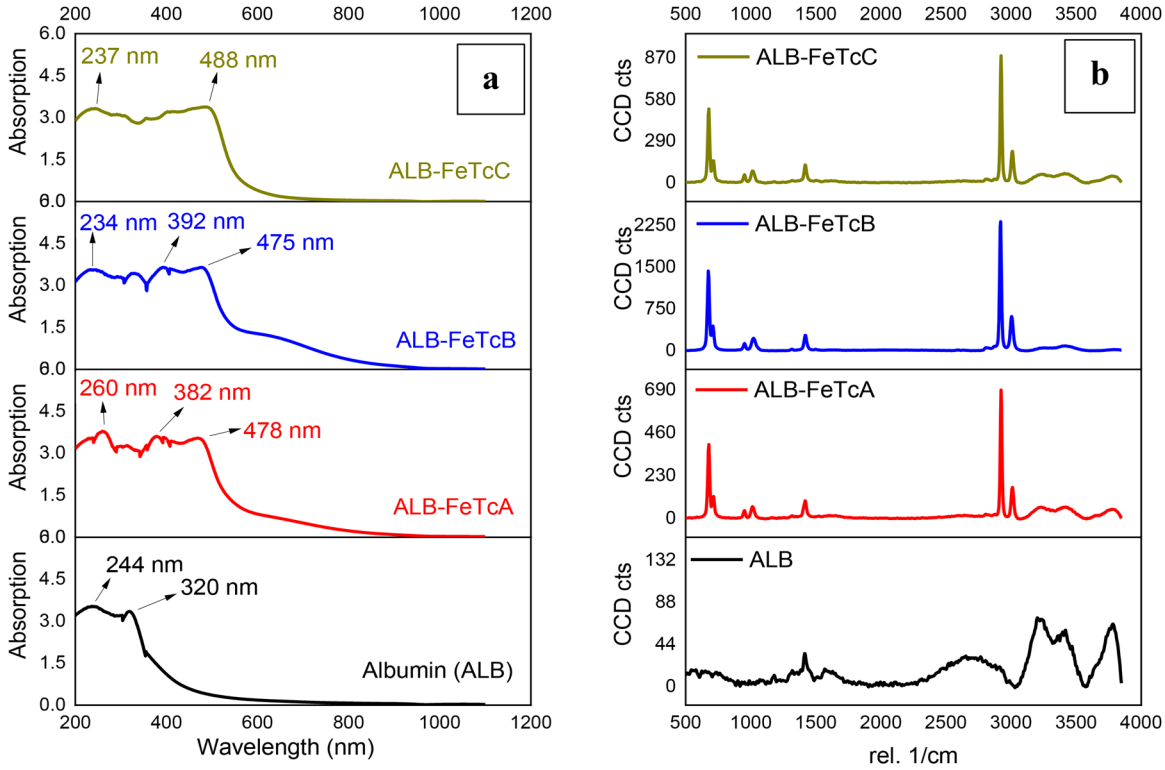

Figure 5. UV-VIS and **b.** Raman spectrum of ALB-FeTcs. In Figure 3b, CCD cts is the CCD detector peak intensity. The real. 1/cm is the wavenumber in the Raman spectrum.

are thought to be responsible for the most significant absorption peak at 260 nm, this depends on the solvent environment of the metal and the thiosemicarbazone attached to the structure. The highest absorption peak at 244 nm moved to 234-237-260 nm due to thiosemicarbazone binding to albumin. The 320 nm emission peak is no longer visible. Instead, at 382–392 nm, emission peaks were visible. Furthermore, around 475-478-488 nm, specific absorption peaks (d-d transitions) associated with FeTcs were also detected. According to all of these studies [39–41], the drug binds to albumin successfully.

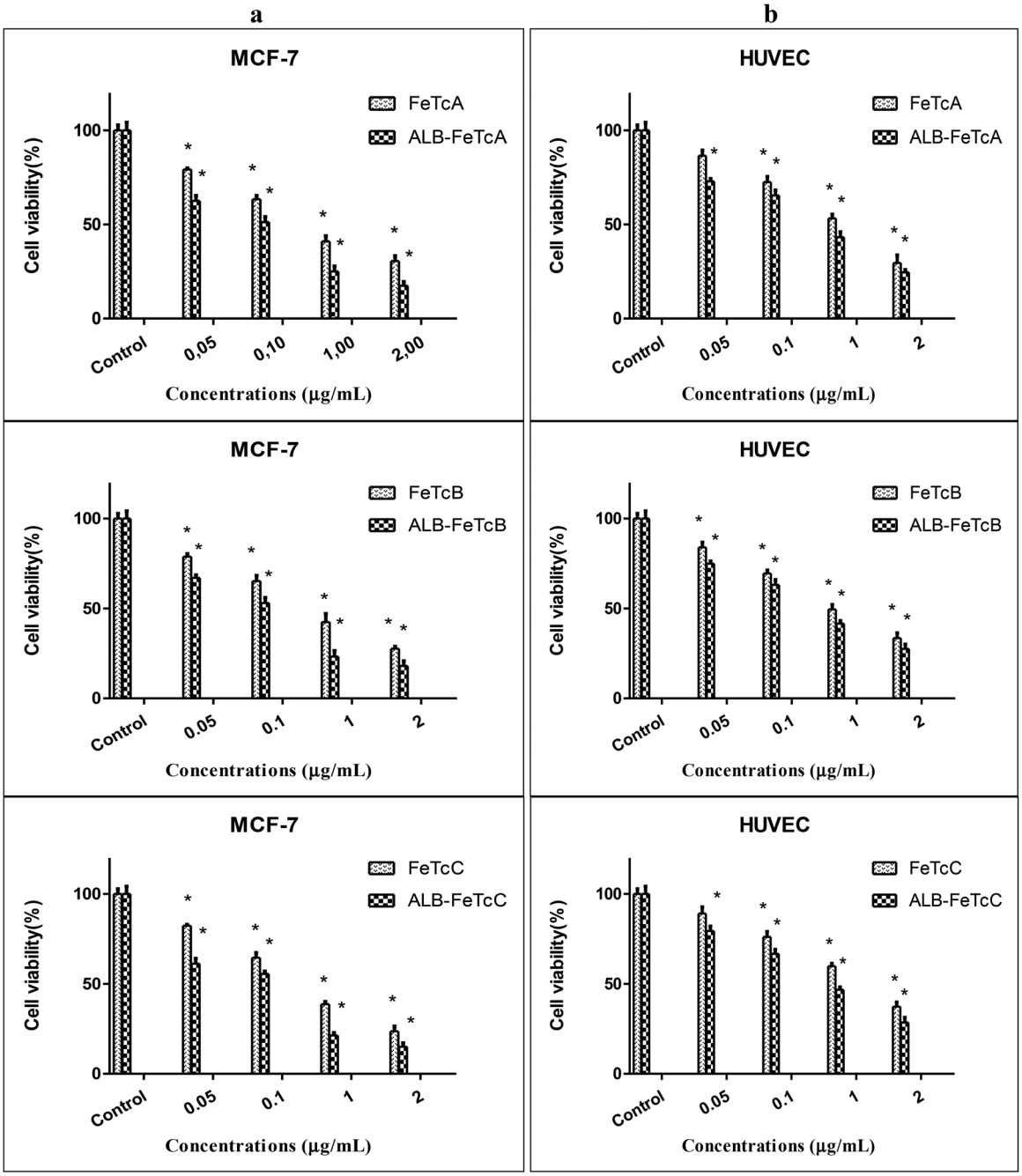

Figure 6. Effects of FeTcA, FeTcB, FeTcC and ALB-FeTcA, ALB-FeTcB, ALB-FeTcC on **(a)** MCF-7 and **(b)** HUVEC cell viability. Cell viability experiments were performed with the MTT test after 72 hours of incubation. The data was analyzed by the GraphPad PRISM 5. Student's t-test was used to determine the significance of the difference between the FeTcA, FeTcB, and FeTcC groups and the ALB-FeTcA, ALB-FeTcB, and ALB-FeTcC groups in comparison to the control groups. Comparisons with a "P" value < 0.05 were considered significant. The concentrations were compared to the control in each group and given as the mean $^{*}P < 0.05$.

The results of the Raman spectrum are shown in Fig. 5b. While bulk albumin and Tc-Metal complexes differed, ALB-FeTcA-B-C did not differ significantly. Because of the remarkable similarity between the functional groups in these three complexes, there is no appreciable difference in Raman vibration spectroscopy. On the other hand, long-term efficacy also depends on the stability of the nanostructure [42]. To establish the long-term efficacy of the cytotoxic analyses, they were scheduled for 72 hours in this investigation.

Thiosemicarbazone ligands are drugs against cancer that bind metal ions and have demonstrated anticancer action in various *in vitro* and *in vivo* studies, including several clinical studies [43–47]. In a study, it was preferred to create HSA complexes to deliver metal drugs because they prevent the introduction of exogenous chemical linkers and the exposure of metal pharmaceuticals to other chemicals and proteins during blood circulation. It was discovered that while the HSA – metal agent complex remains stable in circulation, the metal agent can be liberated in an acidic environment like

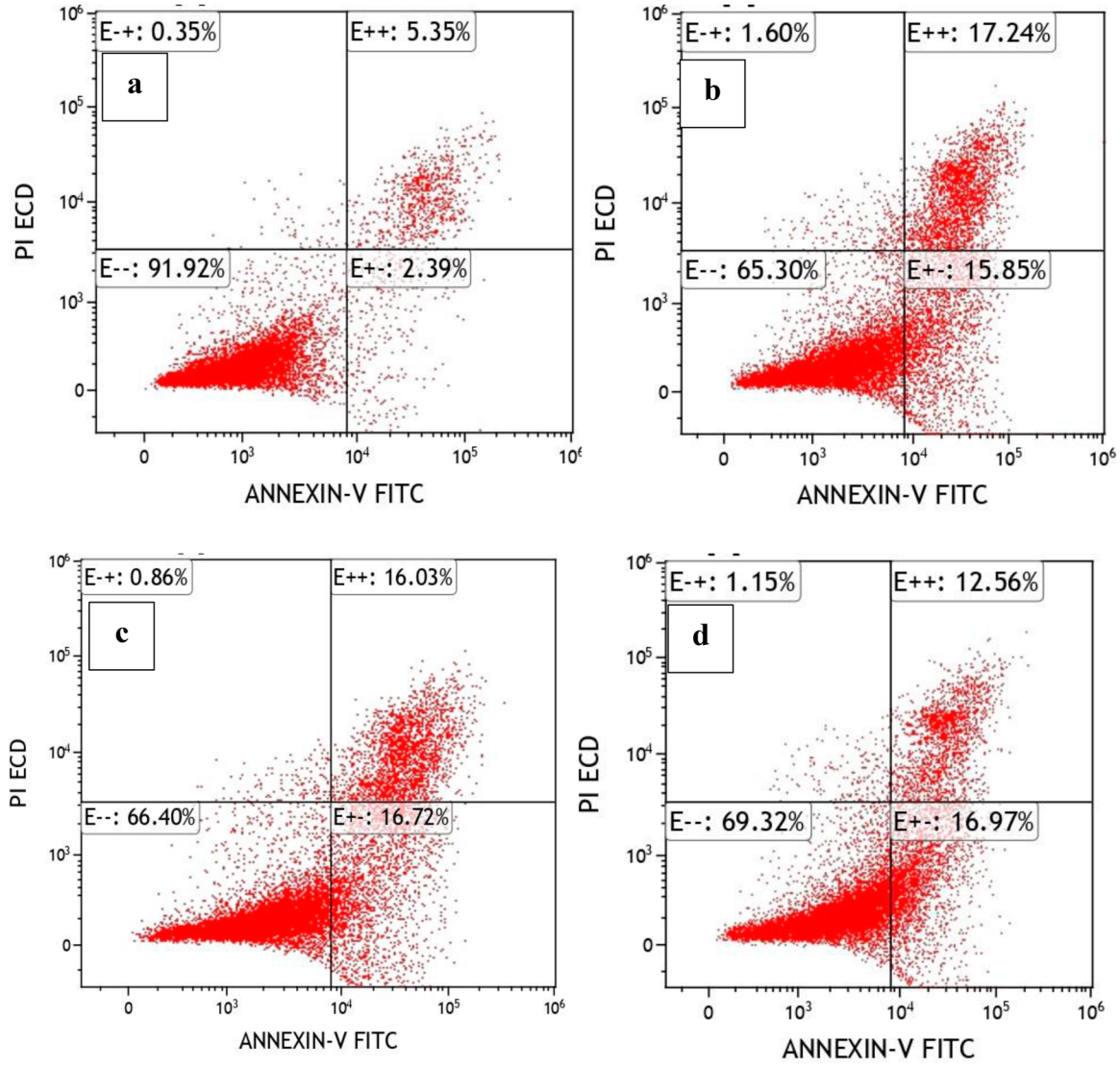

Figure 7. Apoptotic effects of Alb-FeTcA, Alb-FeTcB, and Alb-FeTcC compounds on MCF-7 cells. (**a)** Control, (**b)** Alb-FeTcA, (**c)** Alb-FeTcB and (**d)** Alb-FeTcC. The compounds were evaluated in MCF-7 cells at IC_{50} values by flow cytometry after 72 hours of incubation.

cancer cells. Furthermore, *in vivo* findings demonstrated that the HSA complex was more selective and had higher therapeutic efficiency than metal thiosemicarbazone alone [48]. In this study, to increase the metal complex activity, the iron thiosemicarbazone complex was loaded onto the albumin nanocarrier, and *in vitro* analyses were performed. Accordingly, it was observed that all ALB-FeTc compounds reduced cell viability to below 50% at a dose of 0.1 μg/mL in MCF-7 breast cancer cells (Fig. 6a). Accordingly, when all spectroscopic results are examined in the GraphPad Prism5 program, The IC_{50} value of Alb-FeTcA was found to be 0.1 μg/mL, Alb-FeTcB was 0.19 μg/mL, and Alb-FeTcC was 0.25 μg/mL. As seen in Figure 4, FeTcA is found to be more toxic than FeTcB and FeTcC at lower doses on its own. Hence, its loaded form onto albumin nanocarrier is also found to be more toxic. Due to its chemical structure, it damages the MCF-7 cells more strongly or more quickly. When Fig. 6b is examined, it was determined that the 0.05 μg/mL dose of all ALB-FeTc groups in healthy HUVEC cells reduced cell viability by at most 20%. For a substance to be considered "cytotoxic," it must kill more than 30% of cells compared with the control (EN ISO 19993-5:2009); in our study, any lower dosages of ALB-FeTc-treated groups were not found at the IC_{50} concentration to affect HUVECs to this extent. However, cell proliferation did not significantly increase compared to the control group. This finding suggests that ALB-FeTc compounds were effective at deficient concentrations. In addition, their effectiveness at higher concentrations in healthy HUVEC cells is significant for the feasibility of anticancer treatment. The concept is that albumin nanocarriers infiltrate and aggregate in solid tumors and inflammatory joints by utilizing both the EPR effect and active targeting. The "desire" for albumin, a protein that is necessary for the survival and growth of tumors, is another factor that contributes to the increased accumulation of albumin nanoparticles in solid tumors, in addition to the existence of leaking vasculature and poor lymphatic drainage. Further patient data is required to support the involvement of this mechanism. Similar to cancer

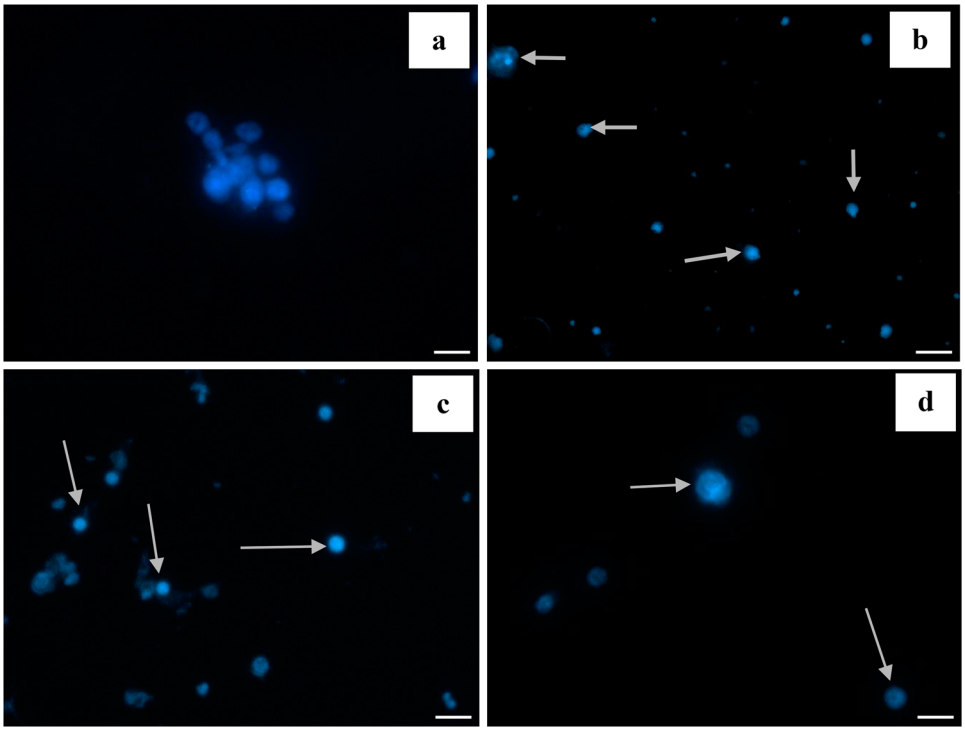

Figure 8. The use of DAPI labeling to identify apoptotic cells of Alb-FeTcA, Alb-FeTcB, and Alb-FeTcC treated MCF-7 cells by fluorescence microscopy. **a.** Control is spherical in shape and is shown as less brightly blue. **b.** Alb-FeTcA, **c.** Alb-FeTcB, **d.** Alb – FeTcC, apoptotic cells exhibit brilliant staining along with other hallmarks of apoptosis, including chromatin condensation, nuclear fragmentation, and the formation of apoptotic bodies. Compounds were applied at IC_{50} values for 72 hours.

patients, rheumatoid arthritis patients frequently experience hypoalbuminemia, which is brought on by the increased albumin consumption in the inflammatory areas. Cachexia is a multifactorial phenomenon characterized by significant weight loss and muscular atrophy. It is associated with all clinical diseases, including cancer, infections, and autoimmune disorders, that promote albumin accumulation in the affected tissue. These considerations make it worthwhile to explore whether the accumulation of injectable albumin-based formulations – regardless of the medications they contain – may either lessen or accelerate the growth of tumors [34]. Because of treatment success, it has also been shown that albumin can be used for selective cellular targeting when different drug combinations are used [47]. Docetaxel and IR780, a near-infrared dye, are combined to create multifunctional HSA NPs. Castration-resistant prostate cancer may be treated with this formulation because of its robust targeting and theranostic potential [49]. In a different study, stimuli-responsive albumin nanoplatforms for multimodal cancer therapy and combined theranostic therapy are also produced. In order to accomplish both the diagnostic and the treatment, multimode therapy works in tandem with imaging technology and depends on chemotherapy, radiotherapy, hypothermia, and other treatments [50]. It has also been said that albumin carrier nanostructures of combined 2-acetylpyridine-4,4-dimethyl-3-thiosemicarbazone-copper(II) [Cu(Ap44mT)]Cl and paclitaxel achieve these properties by suppressing angiogenesis in the tumor microenvironment [51]. For these reasons, we think these compounds loaded on albumin may be a new hope for cancer treatment.

In line with the cytotoxicity results, we examined the apoptosis/necrosis rates in cell death by flow cytometry to determine how Alb-FeTcA, Alb-FeTcB, and Alb-FeTcC nanoparticles cause cell death. As a result, we found that Alb-ZnTcs generally caused cell death through the apoptosis pathway (Fig. 7). Most chemotherapeutic drugs induce apoptosis by altering DNA synthesis and proliferation in cancer cells. Changes in apoptosis sensitivity following medication treatment are suggested to be a significant mechanism in acquired drug resistance. Based on this evidence, it is believed that one of the most significant goals of cancer medication therapy is to promote the apoptotic process for malignant cells [24, 37, 42, 52–54]. It is seen that early apoptotic cells were found to be 17.24%, 16.03%, and 12.56% while late apoptotic cells were detected as 15.85%, 16.72%, and 16.97% in Fig. 7b-d, respectively. In Fig. 7, MCF-7 cells were incubated with Alb-FeTcA, Alb-FeTcB, and Alb-FeTcC nanoparticles at IC_{50} values separately for 72 hours, and as a result, it can be seen that necrosis is almost not observed in cell death in all cell groups, and almost all cell death occurs by apoptosis. According to these findings, the prepared nanostructures increase apoptosis in breast cancer cells.

Fig. 8 shows fluorescence microscopy images of Alb-FeTcA, Alb-FeTcB, and Alb-FeTcC in MCF-7 cells stained with DAPI to see the effects on cell DNA. Since DAPI staining provides the opportunity to visualize cell DNA, it provides information about apoptosis in the cell. In Fig. 8b-d, it is seen that the cells undergo apoptosis compared to the control. Our findings are compatible with the apoptosis results we evaluated by flow cytometry. In a study, a novel In (III) quinoline-2-formaldehyde thiosemicarbazone compound (C5) based on the unique property of human serum albumin (HSA) nanoparticles (NPs) was developed, and fluorescence imaging under *in vivo* conditions detected the PI3K – Akt signaling pathway in tumor cells. It has been found that it inhibits and causes apoptosis [55]. Thus, the importance of cellular targeting has been determined.

4. Conclusion

In this study, Albumin-Bound Fe(III)-S-Methyl-Thiosemi carbazones were successfully synthesized, and their anticancer effects were examined. These NPs enhanced the anticancer activity of Fe(III)-S-Methyl-Thiosemicarb azones on breast cancer cells. In contrast, when ALB-FeTCs were administered in similar concentrations, there was no discernible effect on healthy HUVEC cells. Our results indicate that ALB-FeTCs may be a promising candidate for breast cancer treatment. However, the study did not evaluate the long-term effects of the nano drugs. Therefore, further research is needed to understand the long-term effects of the drugs at *in vivo* conditions and standardize the method.

Disclosure statement

No potential conflict of interest was reported by the author(s).

Funding

This work was supported by Bilimsel Araştırma Projeleri, Erciyes Üniversitesi: [grant number].

ORCID

Dilşad Özerkan http://orcid.org/0000-0002-0556-3879

References

[1] Harbeck N, Penault-Llorca F, Cortes J, et al. Breast cancer. Nat Rev Dis Primers. 2019;5:66. doi:10.1038/s41572-019-0111-2

[2] Siegel Mph RL, Giaquinto AN, Dvm J, et al. Cancer Statistics. 2024;74; doi:10.3322/caac.21820

[3] Ashrafizadeh M, Zarrabi A, Bigham A, et al. (Nano)platf orms in breast cancer therapy: drug/gene delivery, advanced nanocarriers and immunotherapy. Med Res Rev. 2023;43:2115–2176. doi:10.1002/med.21971

[4] Richardson D, Kaya B. Designing Tailored Thiosemicarbazones with Bespoke Properties: The Styrene Moiety Imparts Potent and Selective Anti-Tumor Activity, (2023). https://jpet.aspetjournals.org/content/385/S3/37.abstract (accessed December 19, 2023).

[5] Gregory H, Jensen TR, Pettinari C, et al. Trivalent cobalt complexes with NNS tridentate thiosemicarbazones: preparation, structural study and investigation of antibacterial activity and cytotoxicity against human breast cancer cells. Inorganics. 2022;10(10):145), doi:10.3390/INORGANICS10090145

[6] Asadipour E, Asgari M, Mousavi P, et al. Nano-biotechnol ogy and challenges of drug delivery system in cancer treatment pathway: review article. Review Article, Chem Biodivers. 2023;20:e202201072), doi:10.1002/cbdv.202201072

[7] Haghighi SM, Tafvizi F, Mirzaie A. Encapsulation of artemisia scoparia extract in chitosan-myristate nanogel with enhanced cytotoxicity and apoptosis against hepatocellular carcinoma cell line (Huh-7). Ind Crops Prod. 2020;155:112790), doi:10.1016/j.indcrop.2020.112790

[8] Rezaie Amale F, Ferdowsian S, Hajrasouliha S, et al. Gold nanoparticles loaded into niosomes: A novel approach for enhanced antitumor activity against human ovarian cancer. Adv Powder Technol. 2021;32:4711–4722. doi:10.1016/j.apt.2021.10.019

[9] Haddadian A, Robattorki FF, Dibah H, et al. Niosomes-loaded selenium nanoparticles as a new approach for enhanced antibacterial, anti-biofilm, and anticancer activities. Sci Rep. 2022;12:1–16. doi:10.1038/s41598-022-26400-x

[10] Santhosh P, Mukhtar LA, Kamaraj M, et al. Phytomediated synthesis of copper oxide nanoparticles from floating fern salvinia cucullata roxb. and their antibacterial, antioxidant, and anticancer potential. Biomass Convers Biorefin. 2023;7:1–15. doi:10.1007/S13399-023-04700-0/FIGURES/11

[11] Abirami P, Sampath S, Al-Ansari MM, et al. One-pot synthesis of Ag-Cr bimetallic nanoparticles from catharanthus roseus for anti-bacterial, anticancer, anti-diabetic, and anti-inflammatory activity and toxicity study in zebrafish. Biomass Convers Biorefin. 2023;1:1–15. doi:10.1007/S13399-023-04767-9/FIGURES/11

[12] Balasubramanian A, Ganesan R, Mohanta YK, et al. Characterization of bioactive fatty acid metabolites produced by the halophilic idiomarina sp. OM679414.1 for their antimicrobial and anticancer activity. Biomass Convers Biorefin. 2023;1:1–10. doi:10.1007/S13399-023-04687-8/FIGURES/7

[13] Pourmoghadasiyan B, Tavakkoli F, Beram FM, et al. Nanosized paclitaxel-loaded niosomes: formulation, in vitro cytotoxicity, and apoptosis gene expression in breast cancer cell lines. Mol Biol Rep. 2022;49:3597–3608. doi:10.1007/s11033-022-07199-2

[14] Hassanin I, Elzoghby A. Resistance, undefined 2020, Albumin-based nanoparticles: A promising strategy to overcome cancer drug resistance, Ncbi.Nlm.Nih.Govl Hassanin, A ElzoghbyCancer Drug Resistance, 2020•ncbi. Nlm.Nih.Gov (n.d.). https://www.ncbi.nlm.nih.gov/pmc/articles/PMC8992568/ (accessed December 19, 2023).

[15] Vaz J, Ansari D, Sasor A, et al. SPARC: A potential prognostic and therapeutic target in pancreatic cancer, Pancreas, 2015. https://www.ncbi.nlm.nih.gov/pmc/articles/PMC4568900/ (accessed December 19, 2023).

[16] F.K.-J. of controlled release, undefined 2014, A clinical update of using albumin as a drug vehicle—A commentary, Elsevier (n.d.). https://www.sciencedirect.com/science/article/pii/S0168365914001473 (accessed December 19, 2023).

[17] Bigham A, Aghajanian A. undefined 2019, Nanostructured magnetic Mg2SiO4-CoFe2O4 composite scaffold with multiple capabilities for bone tissue regeneration, Elsevier (n.d.). https://www.sciencedirect.com/science/article/pii/S092849311833515X (accessed December 19, 2023).
[18] Sharifi E, Bigham A, Yousefiasl S, et al. Mesoporous bioactive glasses in cancer diagnosis and therapy: stimuli-responsive, toxicity, immunogenicity, and clinical translation. Wiley Online Library. 2021;9; doi:10.1002/advs.202102678
[19] Jafari Z, Bigham A, Sadeghi S, et al. Nanotechnology-Abetted astaxanthin formulations in multimodel therapeutic and biomedical applications. J Med Chem. 2022;65:2–36. doi:10.1021/ACS.JMEDCHEM.1C01144
[20] Mendes R, Pedrosa P, Lima J. undefined 2017, Photothermal enhancement of chemotherapy in breast cancer by visible irradiation of Gold Nanoparticles, Scientific Reports, 2017•nature.Com (n.d.). https://www.nature.com/articles/s41598-017-11491-8 (accessed December 19, 2023).
[21] Kumari S, Sharma N, Sahi SV, et al. Advances in cancer therapeutics: conventional thermal therapy to nanotechnology-based photothermal therapy. Pharmaceutics. 2021. doi:10.3390/pharmaceutics13081174
[22] Doughty ACV, Hoover AR, Layton E, et al. Nanomaterial applications in photothermal therapy for cancer. Materials (Basel). 2019. doi:10.3390/ma12050779
[23] Johari B, Rahmati M, Nasehi L, et al. Evaluation of STAT3 decoy oligodeoxynucleotides' synergistic effects on radiation and/or chemotherapy in metastatic breast cancer cell line. Cell Biol Int. 2020;44:2499–2511. doi:10.1002/cbin.11456
[24] Johari B, Parvinzad Leilan M, Gharbavi M, et al. Combinational therapy with Myc decoy oligodeoxynucleotides encapsulated in nanocarrier and X-irradiation on breast cancer cells. Oncol Res. 2024;32:309), doi:10.32604/or.2023.043576
[25] Kalındemirtaş FD, Kariper İA, Sert E, et al. The evaluation of anticancer activity by synthesizing 5FU loaded albumin nanoparticles by exposure to UV light. Toxicol in Vitro. 2022;84:105435), doi:10.1016/j.tiv.2022.105435
[26] Mosmann T. Rapid colorimetric assay for cellular growth and survival: application to proliferation and cytotoxicity assays. J Immunol Methods. 1983;65:55–63. doi:10.1016/0022-1759(83)90303-4
[27] Hong JF, Song YF, Liu Z, et al. Anticancer activity of taraxerol acetate in human glioblastoma cells and a mouse xenograft model via induction of autophagy and apoptotic cell death, cell cycle arrest and inhibition of cell migration. Mol Med Rep. 2016;13:4541–4548. doi:10.3892/mmr.2016.5105
[28] Wallberg F, Tenev T, Meier P. Analysis of apoptosis and necroptosis by fluorescence-activated cell sorting. Cold Spring Harb Protoc. 2016. doi:10.1101/PDB.PROT087387
[29] Sibuh BZ, Kumar Gupta P, Taneja P, et al. Synthesis, in silico study, and anti-cancer activity of thiosemicarbazone derivatives. Biomedicines. 2021: 1375), doi:10.3390/biomedicines9101375
[30] Wen Z, Liu F, Liu G, et al. undefined 2021, Assembly of multifunction dyes and heat shock protein 90 inhibitor coupled to bovine serum albumin in nanoparticles for multimodal photodynamic, Elsevier (n.d.). https://www.sciencedirect.com/science/article/pii/S002197972100062X (accessed December 19, 2023).
[31] Zhao W, Li T, Long Y, et al. Self-promoted albumin-based nanoparticles for combination therapy against metastatic breast cancer via a hyperthermia-induced "platelet bridge,". ACS Appl Mater Interfaces. 2021;13:25701–25714. doi:10.1021/acsami.1c04442
[32] Wang D, Li H, Chen W, et al. undefined 2021, Efficient tumor-targeting delivery of siRNA via folate-receptor mediated biomimetic albumin nanoparticles enhanced by all-trans retinoic acid, Elsevier (n.d.). https://www.sciencedirect.com/science/article/pii/S0928493120335013 (accessed December 20, 2023).
[33] Peer D, Karp JM, Hong S, et al. Nano-Enabled medical applications. Nano-Enabled Medical Applications. 2020:61–91. doi:10.1201/9780429399039-2
[34] Spada A, Emami J, Tuszynski JA, et al. The uniqueness of albumin as a carrier in nanodrug delivery. Mol Pharm. 2021;18:1862–1894. doi:10.1021/acs.molpharmaceut.1c00046
[35] Bhushan B, Dubey P, Kumar S, et al. undefined 2015, Bionanotherapeutics: niclosamide encapsulated albumin nanoparticles as a novel drug delivery system for cancer therapy, Pubs.Rsc.OrgB Bhushan, P Dubey, SU Kumar, A Sachdev, I Matai, P GopinathRSC Advances, 2015•pubs.Rsc.Org (n.d.). https://pubs.rsc.org/en/content/articlehtml/2015/ra/c4ra15233f (accessed December 19, 2023).
[36] Sripriyalakshmi S, Jose P, Ravindran A, et al. Recent trends in drug delivery system using protein nanoparticles. Cell Biochem Biophys. 2014;70:17–26. doi:10.1007/s12013-014-9896-5
[37] Cui M, Naczynski DJ, Zevon M, et al. Multifunctional albumin nanoparticles as combination drug carriers for intra-tumoral chemotherapy. Adv Healthcare Mater, 2013;2:1236–1245. doi:10.1002/adhm.201200467.
[38] Zawisza K, Sobierajska P, Nowak N, et al. undefined 2020, Preparation and preliminary evaluation of bionanocomposites based on hydroxyapatites with antibacterial properties against anaerobic bacteria, Elsevier (n.d.). https://www.sciencedirect.com/science/article/pii/S092849311832616X (accessed December 20, 2023).
[39] Jiao C, Zhang SS, Li ZY, et al. Syntheses and structures of discrete copper(II) and cadmium(II) supramolecular complexes based on 1,4-diacylthiosemicarbazone ligands. Acta Crystallogr C Struct Chem. 2016;72:119–123. doi:10.1107/S2053229616000310
[40] Hricovíni M, Mazúr M, Sîrbu A, et al. Molecules, undefined 2018, Copper (II) thiosemicarbazone complexes and their proligands upon uva irradiation: An epr and spectrophotometric steady-state study, Mdpi.ComM Hricovíni, M Mazúr, A Sîrbu, O Palamarciuc, VB Arion, V Brezová-Molecules, 2018•mdpi.Com (n.d.). https://www.mdpi.com/1420-3049/23/4/721 (accessed December 19, 2023).
[41] D Polo-CeronBioinorganic. Chemistry and applications, undefined 2019, Cu (II) and Ni (II) complexes with new tridentate NNS thiosemicarbazones: Synthesis, characterisation, DNA interaction, and antibacterial activity, Hindawi.Com Chemistry and Applications, 2019•hindawi.Com (n.d.). https://www.hindawi.com/journals/bca/2019/3520837/ (accessed December 19, 2023).
[42] Zhao P, Yin W, Wu A, et al. Dual-Targeting to cancer cells and M2 macrophages via biomimetic delivery of mannosylated albumin nanoparticles for drug-resistant cancer therapy, Wiley Online Library 27 2017. doi:10.1002/adfm.201700403.
[43] Buss J, Torti F, Torti SV. Current medicinal chemistry, undefined 2003, The role of iron chelation in cancer therapy, Ingentaconnect.Com Current Medicinal Chemistry, 2003•ingentaconnect.Com (n.d.). https://www.ingenta

connect.com/content/ben/cmc/2003/00000010/00000012/art00005 (accessed December 19, 2023).

[44] Yen Y, Margolin K, Doroshow J, et al. A phase I trial of 3-aminopyridine-2-carboxaldehyde thiosemicarbazone in combination with gemcitabine for patients with advanced cancer. Cancer Chemother Pharmacol. 2004;54:331–342. doi:10.1007/S00280-004-0821-2

[45] Wadler S, Makower D, Clainmont C, et al. Phase I and pharmacokinetic study of the ribonucleotide reductase inhibitor, 3-aminopyridine-2-carboxaldehyde thiosemicarbazone, administered by 96-hour intravenous continuous infusion. J Clin Oncol. 2004;22:1553–1563. doi:10.1200/JCO.2004.07.158

[46] Kalinowski D. D.R.-P. reviews, undefined 2005, The evolution of iron chelators for the treatment of iron overload disease and cancer, ASPETDS Kalinowski, DR RichardsonPharmacological Reviews, 2005•ASPET (n.d.). https://pharmrev.aspetjournals.org/content/57/4/547.short (accessed December 19, 2023).

[47] Merlot A, Sahni S, Lane D. A.F.- Oncotarget, undefined 2015, Potentiating the cellular targeting and anti-tumor activity of Dp44mT via binding to human serum albumin: two saturable mechanisms of Dp44mT uptake by, Ncbi.Nlm.Nih.GovAM Merlot, S Sahni, DJR Lane, AM Fordham, N Pantarat, DE Hibbs, V RichardsonOncotarget, 2015•ncbi.Nlm.Nih.Gov (n.d.). https://www.ncbi.nlm.nih.gov/pmc/articles/PMC4496362/ (accessed December 19, 2023).

[48] Yang F, Liang H. Designing anticancer multitarget metal thiosemicarbazone prodrug based on the nature of binding sites of human serum albumin carrier. Future Med Chem. 2018;10:1881–1883. doi:10.4155/fmc-2018-0175

[49] Lian H, Wu J, Hu Y, et al. Self-assembled albumin nanoparticles for combination therapy in prostate cancer. Int J Nanomedicine. 2017;Volume 12:7777–7787. doi:10.2147/IJN.S144634

[50] Li C, Wang X, Song H, et al. Current multifunctional albumin-based nanoplatforms for cancer multi-mode therapy. Asian J Pharm Sci. 2020;15:1–12. doi:10.1016/j.ajps.2018.12.006

[51] Zhang Z, Zhang J, Jiang M, et al. Human serum albumin-based dual-agent delivery systems for combination therapy: acting against cancer cells and inhibiting neovascularization in the tumor microenvironment. Mol Pharm. 2020;17:1405–1414. doi:10.1021/acs.molpharmaceut.0c00133

[52] Battogtokh G, Gotov O, Kang JH, et al. Triphenylphosphine-docetaxel conjugate-incorporated albumin nanoparticles for cancer treatment. Nanomedicine. 2018;13:325–338. doi:10.2217/nnm-2017-0274

[53] Khella K, El Maksoud AA. Molecules, undefined 2022, Carnosic acid encapsulated in albumin nanoparticles induces apoptosis in breast and colorectal cancer cells, Mdpi.ComKF Khella, AI Abd El Maksoud, A Hassan, SE Abdel-Ghany, RM Elsanhoty, MA AladhadhMolecules, 2022•mdpi.Com (n.d.). https://www.mdpi.com/1420-3049/27/13/4102 (accessed December 19, 2023).

[54] Yurt F, Özel D, Tunçel A, et al. Synthesis and optimization of the docetaxel-loaded and durvalumab-targeted human serum albumin nanoparticles, In vitro characterization on triple-negative breast cancer cells. ACS Omega. 2023;8:26287–26300. doi:10.1021/ACSOMEGA.3C02682

[55] Zhang Z, Yang T, Zhang J, et al. Developing a novel indium(III) agent based on human serum albumin nanoparticles: integrating bioimaging and therapy. J Med Chem. 2022;65:5392–5406. doi:10.1021/acs.jmedchem.1c01790